Improving the Signal Sensitivity and Photostability of DNA Hybridizations on Microarrays by Using Dye-Doped Core−Shell Silica Nanoparticles

Xichun Zhou and Jizhong Zhou*

Microbial Genomics and Ecology Group, Environmental Science Division, Oak Ridge National Laboratory, Oak Ridge, Tennessee 37831

The development of new highly sensitive and selective methods for microarray-based analysis is a great challenge because, for many bioassays, the amount of genetic material available for analysis is extremely limited. Currently, imaging and detection of DNA microarrays are based primarily on the use of organic dyes. To overcome the problems of photobleaching and low signal intensities of organic dyes, we developed a new class of silica core−shell nanoparticles that encapsulated with cyanine dyes and applied the dye-doped nanoparticles as labeling in the DNA microarray-based bioanalysis. The developed nanoparticles have core−shell structure containing 15-nm Au colloidal cores with 95 dye−alkanethiol (dT)$_{20}$ oligomers chemisorbed on the each Au particle surface and 10−15-nm silica coatings bearing thiol functional groups. To be utilized for microarray detection, the dye-doped nanoparticles were conjugated with DNA signaling probes by using heterobifunctional cross-linker. The prepared nanoparticle conjugates are stable in both aqueous electrolytes and organic solvents. Two-color DNA microarray-based detection was demonstrated in this work by using Cy3- and Cy5-doped nanoparticles in sandwich hybridization. The use of the fluorophore-doped nanoparticles in high-throughput microarray detection reveals higher sensitivity with a detection limit of 1 pM for target DNA in sandwich hybridization and greater photostable signals than the direct use of organic fluorophore as labeling. A wide dynamic range of ∼4 orders of magnitude was also found when the dye-doped nanoparticles were applied in microarray-based DNA bioanalysis. In addition, the use of these dye-doped nanoparticles as the labeling in hybridization also improved the differentiation of single-nucleotide polymorphisms. This work offers promising prospects for applying dye-doped nanoparticles as labeling for gene profiling based on DNA microarray technology.

The recent advent of high-throughput technologies such as microarrays and microanalytical devices has provided unprecedented convenience and capability for genotyping and detecting microorganisms.[1,2] Currently, most microarray imaging and analysis are primarily based on the use of fluorescence from organic fluorophores. However, the use of organic fluorophores suffers from photobleaching, low signal intensities, spectral overlaps, and random on/off emissions (blinking).[3,4] Organic fluorophores are also not stable in the ambient environment. Fare et al. reported that fluorophores, especially the cyanine dyes (e.g., Cy5, Alexa 647), showed significant degradation in the laboratory when microarrays were exposed to ozone levels of 5−10 ppb for periods as short as 1 min.[5] This degradation significantly affects the uniformity and reproducibility of fluorescent signals across DNA microarrays. It is highly demanded to achieve strong and photostable fluorescence signals for microarray-based bioanalysis. Moreover, because the amount of genetic materials available for analysis is extremely limited and the reaction volumes used are in the microliter or nanoliter range,[6−8] it is also important to develop highly sensitive and selective methods for microarray-based analysis.

Recently, progress has been made toward more sensitive analysis with photostable signals using novel labeling approaches in bioanalysis and imaging technology, such as resonance light scattering particles,[7] near-infrared dyes,[9] up-converting phosphors,[10,11] fluorophore-doped nanoparticles[12−17] and quantum

* Corresponding author. Phone: (865) 576-7544. Fax: (865) 576-8646. E-mail: zhouj@ornl.gov.

(1) van Ingen, C. *Nat. Genet.* **2002,** *32,* 463.
(2) Brown, P. O.; Botstein, D. *Nat. Genet.* **1999,** *21,* 33−37.
(3) Ballou, B.; Fisher, G. W.; Deng, J. S.; Hakala, T. R.; Srivastava, M.; Farkas, D. L. *Cancer Detect. Prev.* **1998,** *22,* 251−257.
(4) Colson, S.; Sudar, D. Report on the Imaging Workshop for the Genomes to Life Program, Charlotte, NC, April 16−18, 2002 (http://www.doe genomestolife.org/technology/imaging/workshop 2002/GTLimaging2002.pdf).
(5) Fare, T. L.; Coffey, E. M.; Dai, H. Y.; He, Y. D. D.; Kessler. D. A.; Kilian, K. A.; Koch, J. E.; LeProust, E.; Marton, M. J.; Meyer, M. R.; Stoughton, R. B.; Tokiwa, G. Y.; Wang, Y. Q. *Anal. Chem.* **2003,** *75,* 4672−4675.
(6) Duggan, D. J.; Bittner, M.; Chen, Y.; Meltzer, P.; Trent, J. M. *Nat. Genet.* **1999,** *21,* 10−14.
(7) Bao, P.; Frutos, A. G.; Greef, C.; Lahiri, J.; Muller, U.; Peterson, T. C.; Warden, L.; Xie, X. Y. *Anal. Chem.* **2002,** *74,* 1792−1797.
(8) Celis, J. E.; Kruhoffer, M.; Gromova, I.; Frederiksen, C.; Ostergaard, M.; Thykjaer, T.; Gromov, P.; Yu, J.; Palsdottir, H.; Magnusson, N.; Orntoft, T. F. *FEBS Lett.* **2000,** *480,* 2−16.
(9) Waddell, E.; Wang, Y.; Stryjewski, W.; McWhorter, S.; Henry, A. C.; Evans, D.; McCarley, R. L.; Soper, S. A. *Anal. Chem.* **2000,** *72,* 5907−5917.
(10) Rijke, F. v. d.; Zijlmans, H.; Li, S.; Vail, T.; Raap, A. K.; Niedbala, R. S.; Tanke, H. J. *Nat. Biotechnol.* **2001,** *19,* 273−276.
(11) Hampl, J.; Hall, M.; Mufti, N. A.; Yao, Y. M. M.; MacQueen, D. B.; Wright, W. H.; Cooper, D. E. *Anal. Biochem.* **2001,** *288,* 176−187.
(12) Tapec, R.; Zhao, X. J. J.; Tan, W. H. *J. Nanosci. Nanotechnol.* **2002,** *2,* 405−409.

dots.[18−21] Among these approaches, nanomaterials such as luminescent quantum dots and nanoparticles encapsulated with fluorophores hold great promise. Quantum dots have been proved recently to be a stable luminescent label for imaging technology[18] and microarray-based analysis,[19,20c] but the routine application of quantum dots is still controversial. There are general environmental concerns regarding the use of highly toxic cadmium compounds. Moreover, the luminescent properties of quantum dots are highly dependent on their size and shape. These characteristics add difficulty to the achievement of homogeneous and consistent microarray hybridization when multiple-colored quantum dots (i.e., quantum dots in different sizes and shapes) have to be involved in one hybridization event. Moreover, new scanner systems have to be built up for use of quantum dots or upconverting phosphors as labeling in microarray technology because the conventional scanners in biological laboratories are not equipped with detection channels for the fluorescence from quantum dots or upconverting phosphors. Fluorophore-doped silica nanoparticles (FDSPs) have also been used for imaging and bioanalysis in recent years.[12−17] The FDSPs entrap a large number of fluorophores in a silica matrix. The use of FDSPs as labeling reagents for DNA detection can provide higher sensitivity than dye molecules because hybridization events are signaled directly when a large amount of fluorophores are attached to the DNA probe. The fluorophores of FDSPs are highly photostable and well-protected from environmental oxygen because they are shielded inside a silica matrix; thus, the fluorescence is constant and gives an accurate measurement. However, the reported methods for encapsulation of fluorophores into silica by weak absorption have several drawbacks including poor solubility of the dyes in pure silica, migration, and aggregation of the dyes, which resulted in decreasing fluorescent efficiency and variability in the amount of dye molecules encapsulated in each nanoparticle.[12,14]

In this paper, we described and demonstrated an improved class of cyanine dye-doped Au/silica core−shell nanoparticles for use as highly sensitive and photostable labels in oligonucleotide microarray applications. The nanoparticle contains an Au colloid core conjugated with dye molecules by strong chemisorptions and an encasing silica shell tailed with thiol functional groups for protection of the embedded dye molecules and for bioconjugation of DNA probes onto the shell surface. In contrast to most previous dye-doped nanoparticles, where the fluorophores are randomly encapsulated in silica matrix by weak adsorption,[12−17] in the present work, the dye molecules were conjugated to an Au colloidal core first and then embedded in the silica shell. This design provides a well built-in mechanism to dope nanoparticles and thus avoids the problems of dye leaking and variation of the amount of dye molecules in individual nanoparticles. Both Cy3- and Cy5-doped Au/silica core−shell particles were prepared and applied to two-color microarray detection. The work described here provides the first example of use of dye-doped nanoparticles for multiplexed detection in microarray technology by preparing silica nanoparticles with consistent dye molecules encapsulated in individual nanoparticles.

EXPERIMENTAL SECTION

Most reagents were purchased from Sigma-Aldrich-Fluka Chemical Corp. (Milwaukee, WI) and were used as received: (3-mercaptopropyl)trimethoxysilane (MPTS), tetraethyl orthosilicate (TEOS) (99.999%), ammonium hydroxide (25%), Denhardt's solution (containing 1 mg/mL each of Ficoll, poly(vinylpyrrolidone), and bovine serum albumin), PBS and SSC buffers, ethanol, and acetone. The 2-(methoxypoly(ethyleneoxy)propyl)trimethoxysilane ((PEG)-silane) was purchased from Gelest (Morrisville, PA). The 15-nm-size gold colloids were obtained from Research Diagnostics Inc. (Flanders, NC), and N-[κ-maleimidoundecanoyloxy]sulfosuccinimide ester (sulfo-KMUS) was purchased from Pierce Biotechnology, Inc. (Rockford, IL). Frame-Seal incubation chambers (9 × 9 mm) was obtained from MJ Research Inc. (Watertown, MA). DNA oligomers were synthesized at the Michigan State University Macromolecular Center. Four of 5′-terminal alkylamine-modified oligonucleotide probes, 19-mer of Td1 (*Azoarcus tolulyticus* 16S gene), 21-mer of Heme (incorporating the *Pseudomonas stutzeri* nitrite reductase gene), 21-mer of AmoA (*Nitrosospira sp. Np39-19* ammonia monooxygenase gene), and a 21-mer random probe that was used as a negative control, were used to fabricate an oligonucleotide microarray for the sensitivity test. Another 16 of 5′-terminal alkylamine-modified 21-mer oligonucleotide probes were synthesized and used to fabricate a microarray for the specificity test. The sequences of the oligonucleotide probes and targets are shown in Table 1. Two cyanine dye-labeled oligomers with alkanethiol modifications, 5′-thiolated (dT)$_{20}$−Cy3 and 5′-thiolated (dT)$_{20}$−Cy5, were used to conjugate the Au colloid. Aldehyde-modified slides (SuperAldehyde slides) were purchased from TeleChem International (Sunnyvale, CA).

Preparation of Dye-Doped Silica Nanoparticles and Conjugation of DNA Signaling Probes onto a Nanoparticle Surface (Scheme 1). *Preparation of Cy3- and Cy5-Conjugated Au Nanoparticles.* The coupling of the fluorophore−alkanethiol oligonucleotides to the Au colloids was carried out using a procedure similar to Demers et al.[22] Briefly, 5′-thiolated (dT)$_{20}$−Cy3 or 5′-thiolated (dT)$_{20}$−Cy5 was added to an Au colloidal solution (particle concentration ∼1.4 × 10^{12} particle mL$^{−1}$) to a final oligonucleotide concentration of 0.25 μM. After 16 h, the

(13) Santra, S.; Zhang, P.; Wang, K. M.; Tapec, R.; Tan, W. H. *Anal. Chem.* **2001**, *73*, 4988−4993.

(14) Zhao, X. J.; Tapec-Dytioco, R.; Tan, W. H. *J. Am. Chem. Soc.* **2003**, *125*, 11474−11475.

(15) Hilliard, L. R.; Zhao, X. J.; Tan, W. H. *Anal. Chim. Acta* **2002**, *470*, 51−56.

(16) Qhobosheane, M.; Santra, S.; Zhang, P.; Tan, W. H. *Analyst* **2001**, *126*, 1274−1278.

(17) Taylor, J. R.; Fang, M. M.; Nie, S. M. *Anal. Chem.* **2000**, *72*, 1979−1986.

(18) (a) Gao, X. H.; Chan, W. C. W.; Nie, S. M. *J Biomed. Opt.* **2002**, *7*, 532−537. (b) Jaiswal, J. K.; Mattoussi, H.; Mauro, J. M.; Simon, S. M. *Nat. Biotechnol.* **2003**, *21*, 47−51. (c) Wu, X. Y.; Liu, H. J.; Liu, J. Q.; Haley, K. N.; Treadway, J. A.; Larson, J. P.; Ge, N. F.; Peale, F.; Bruchez, M. P. *Nat. Biotechnol.* **2003**, *21*, 41−46.

(19) (a) Gerion, D.; Chen, F. Q.; Kannan, B.; Fu, A. H.; Parak, W. J.; Chen, D. J.; Majumdar, A.; Alivisatos, A. P. *Anal. Chem.* **2003**, *75*, 4766−4772. (b) Parak, W. J.; Gerion, D.; Zanchet, D.; Woerz, A. S.; Pellegrino, T.; Micheel, C.; Williams, S. C.; Seitz, M.; Bruehl, R. E.; Bryant, Z.; Bustamante, C.; Bertozzi, C. R.; Alivisatos, A. *Chem. Mater.* **2002**, *14*, 2113-2119. (c) Gerion, D.; Parak, W. J.; Williams, S. C.; Zanchet, D.; Micheel, C. M.; Alivisatos, A. P. *J. Am. Chem. Soc.* **2002**, *124*, 7070−7074. (d) Willner, I.; Patolsky, F.; Wasserman, J. *Angew. Chem., Int. Ed.* **2001**, *40*, 1861−1864.

(20) (a) Maxwell, D. J.; Taylor, J. R.; Nie, S. M. *J. Am. Chem. Soc.* **2002**, *124*, 9606−9612. (b) Byassee, T. A.; Chan, W. C. W.; Nie, S. *Anal. Chem.* **2000**, *72*, 5606−5611. (c) Chan W. C. W,; Nie, S. M. *Science* **1998**, *281*, 2016−2018.

(21) Cao, Y. W. C.; Jin, R. C.; Mirkin, C. A. *Science* **2002**, *297*, 1536−1540.

(22) (a) Demers, L. M.; Mirkin, C. A.; Mucic, R. C.; Reynolds, R. A.; Letsinger, R. L. *Anal. Chem.* **2000**, *72*, 5535−5541. (b) Storhoff, J. J.; Elghanian, R.; Mirkin, C. A.; Letsinger, R. L. *Langmuir* **2002**, *18*, 6666−6670.

Table 1. Sequence of the Oligomer Probes Used in This Work[a]

name	sequence (from 5′ to 3′)
Td1	NH_2-$(CH_2)_3$-ACG CGA GGT CTT GCG ATC C
Heme	NH_2-$(CH_2)_3$−CAC GTT GAA CTT ACC GGT CGG
AmoA	NH_2-$(CH_2)_3$-GTG CCG TGA TCA TCC AGT TGC
control	NH_2-$(CH_2)_3$-AGC CGG TGC TTC TTC TGA CAG
Heme-A	NH_2-$(CH_2)_3$−CAC GTT GAA CTT ACC GGT CGG
Heme-B	NH_2-$(CH_2)_3$−CAC GTT GAA C**A**T ACC GGT CGG
Heme-C	NH_2-$(CH_2)_3$−CAC GTT GAA C**C**T ACC GGT CGG
Heme-D	NH_2-$(CH_2)_3$−CAC GTT GAA C**G**T ACC GGT CGG
Heme-E	NH_2-$(CH_2)_3$−CAC GTT GAA **GA**T ACC GGT CGG
Heme-F	NH_2-$(CH_2)_3$−CAC GTT GAA **AA**T ACC GGT CGG
Heme-G	NH_2-$(CH_2)_3$−CAC GTT GAA **TA**T ACC GGT CGG
Heme-H	NH_2-$(CH_2)_3$−CAC GTT GAA **GC**T ACC GGT CGG
Heme-I	NH_2-$(CH_2)_3$−CAC GTT GAA **AC**T ACC GGT CGG
Heme-J	NH_2-$(CH_2)_3$−CAC GTT GAA **TC**T ACC GGT CGG
Heme-K	NH_2-$(CH_2)_3$−CAC GTT GAA **GGC** ACC GGT CGG
Heme-L	NH_2-$(CH_2)_3$−CAC GTT GAA **AGA** ACC GGT CGG
Heme-M	NH_2-$(CH_2)_3$−CAC GTT GAA **TGC** ACC GGT CGG
Heme-N	NH_2-$(CH_2)_3$−CAC GTT GAA **GAC** ACC GGT CGG
Heme-O	NH_2-$(CH_2)_3$−CAC GTT GA**T GAC** ACC GGT CGG
Heme-P	NH_2-$(CH_2)_3$−CAC GTT GA**T** GAC **T**CC GGT CGG
Td1-target	agg ggg aaa gcg gg *GGA TCG CAA GAC CTC GCG T*GA TTG GAG CGG CCG AT
Heme-target	cgg ccg tcg tca ct*C CGA CCG GTA AGT TCA ACG TG*T TCA ACA CCA TGA AC
AmoA-target	cct gct tct gac gc*G CAA CTG GAT GAT CAC GGC AC*T GGT TGG CGG CGG CG
Td1-signaling	ccc gct ttc ccc ct-$(CH_2)_3$−NH_2
Heme- signaling	agt gac gac ggc cg-$(CH_2)_3$−NH_2
AmoA- signaling	gcg tca gaa gca gg-$(CH_2)_3$−NH_2
Cy5-Heme signaling	agt gac gac ggc cg-Cy5

[a] Mismatch base pairs in the probes are underlined and boldface, and the sequence at the DNA targets that was complementary to the probes was in italic and underlined, while the sequence at the DNA targets that was complementary to the signaling probe is in lower case.

Scheme 1. Procedures for Preparing Dye-Doped Core−Shell Nanoparticles and Its Structure[a]
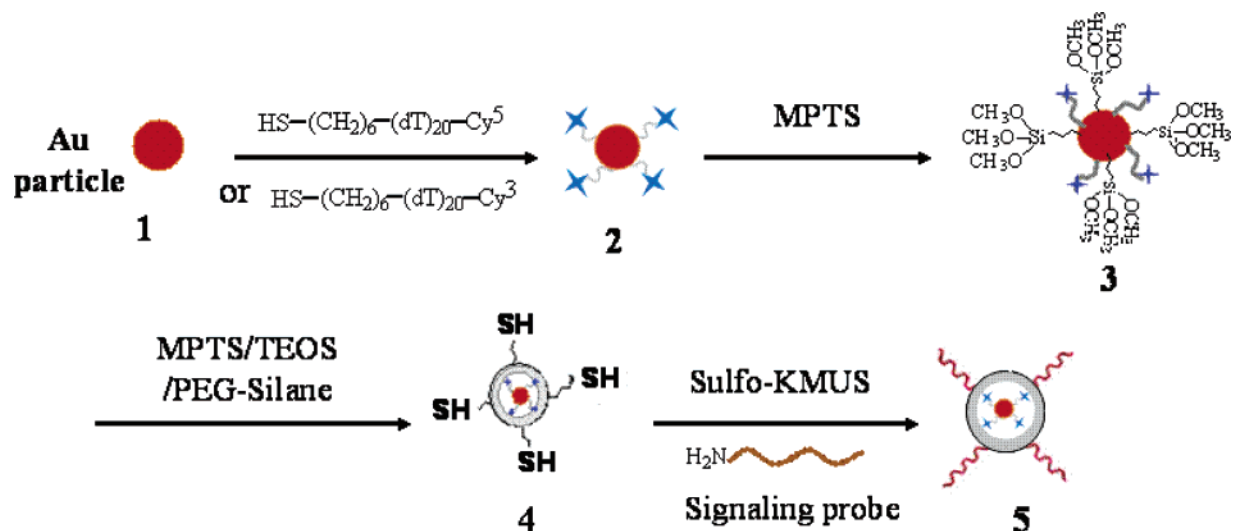
[a] (1) 15 nm of colloidal gold particle; (2) gold colloid conjugated with fluorophore-labeled alkanethiol (dT)$_{20}$; (3) gold colloid adsorbed with both the fluorophore and MPTS; (4) thiol-functionalized silica-coated gold particles with fluorophore embedded in the core−shell boundary; (5) dye-doped core−shell nanoparticle conjugated with DNA signaling probe.

solution was buffered with 1× PBS buffer, followed by aging for 24 h. The nanoparticle conjugates were purified three times by centrifugation at 14 000 rpm for ~10 min. The final product was resuspended and stored in 1× PBS buffer. The conjugation of Cy3- or Cy5-labeled oligonucleotides on Au nanoparticle was confirmed using UV−visible spectroscopy.

The average number of oligonucleotide molecules associated with each Au particle was estimated using the following methodology. The cyanine dye-labeled, oligonucleotide−functionalized Au colloid (250 μL) was treated for 2 h with DNase I (Amersham Pharmacia; 40 units at 37 °C in 40 mM tris-HCl, pH 7.5, in the presence of 6 mM $MgCl_2$). The resulting mixture was centrifuged, and the fluorescence of the cyanine dyes in the supernatant solution was determined using a fluorospectrometer. The gold particle concentration was measured by optical absorbance at 510 nm. The numbers of conjugated dyes (i.e., the conjugated oligonucleotides) per particle were estimated by dividing the total number of dye molecules by the total number of Au nanoparticles.

Synthesis of Dye-Doped Au/Silica Core−Shell Nanoparticles.
Silica core−shell nanoparticles encapsulated with cyanine dye-conjugated Au colloid were prepared as follows: (To avoid possible photobleaching, all the following experiments including synthesis of dye-doped silica nanoparticles and preparation of DNA/nanoparticle conjugates were conducted in dark by wrapping the reaction tube with aluminum film.) Three milliliters of ethanol solution containing 0.5 μM MPTS was added to 3 mL of the dye-conjugated Au colloid solution under stirring. The solution was left to stand for 15 min in order for adsorption and hydrolysis of the methoxysilane groups on the Au surface to form a lattice of siloxane bond around the vitreophilic Au nanoparticles. A shell of organosilica was then synthesized around the primed nanoparticles by cocondensation. Three milliliters of freshly prepared MPTS/TEOS/(PEG)-silane (1:1:1) mixture and 60 μL of NH$_4$OH (25%) in ethanol were added dropwise into the colloidal solution under vigorous stirring, and then the solution was left under mild magnetic stirring for 24 h at room temperature. A shell of silica coating was generated and tailored with thiol as the functional group. Ten milliliters of acetone was added to stop the reaction, and the nanoparticles were isolated by centrifugation and washing with water several times to remove any unreacted reagents. The prepared silica-coated nanoparticles were resuspended in 1× PBS (pH 7.4) at concentration of 2×10^{12} particle mL^{-1}.

Covalent Conjugation of Oligonucleotide Signaling Probes onto the Silica Nanoparticle Surface. The alkylamino-modified DNA signaling probes were conjugated to the thiol-functionalized silica nanoparticles in a two-step procedure using the heterobifunctional cross-linker sulfo-KMUS. For example, 0.5 nmol of alkylamine-modified Td1 capture probe was mixed with 0.5 nmol of sulfo-SMCC in 1 mL of 1× PBS buffer at room temperature for 1 h. The solution was then transferred to 1 mL of the thiol-functionalized Cy3-doped silica nanoparticles and the solution left under mild stirring for 2 h at room temperature. The nanoparticles were washed with 1× PBS three times to remove excess sulfo-KMUS, then treated with 5× Denhardt's solution for 30 min, and washed with 1× PBS buffer. Finally, the resulting Cy3-doped nanoparticles functionalized with Td1 signaling probe (hereafter referred to as Cy3-NP-Td1) were resuspended in 1 mL of 1× SSC (1× SSC contained 150 mM NaCl and 15 mM trisodium citrate), 0.2%SDS solution and either used immediately or stored at 4 °C. The same protocol was used to prepare the Cy3-doped nanoparticles coupled with Heme signaling probe (hereafter referred to as Cy3-NP−Heme), Cy5-doped nanoparticles coupled with Heme signaling probe (hereafter referred to as Cy5-NP−Heme), and Cy5-doped nanoparticles coupled with AmoA signaling probe (hereafter referred to as Cy5-NP−AmoA). Scheme 1 outlines the procedures for preparing dye-doped nanoparticles functionalized with signaling probes.

Gel electrophoresis was used to verify coupling of oligonucleotide signaling probes to nanoparticles. The oligonucleotide-derivatized nanoparticles were diluted in loading buffer containing 10% glycerol and were run in 10 mM PB buffer (pH 2) on a 1% agarose gel at 70 V for 1 h. The gels were illuminated with an UV transilluminator.

The average number of oligonucleotide units associated with each silica nanoparticle was determined by treating a suspension of nanoparticle solution with the Cy5-labeled 16-mer oligonucle-otide Cy5-AGT GAC GAC GGC CG-(CH$_2$)$_3$-NH$_2$ under the same protocol as described above. A 250-μL sample of the resulting Cy5-labeled, oligonucleotide-functionalized silica nanoparticle (2×10^{12} particle mL^{-1},) was treated for 2 h with 20 units of DNase I at 37 °C. The resulting mixture was centrifuged, and the solution containing released Cy5 fluorophores was separated from the silica nanoparticle aggregates. The fluorescence of the Cy5 in the supernatant solution was measured by fluorescence spectroscopy, and the concentration of Cy5 fluorophores, which is equal to the coupled oligonucleotides, was calculated from the Cy5 standard curve.

Measurements and Characterization. UV adsorption spectra were acquired by using the HP 845 UV−visible system, and fluorescent spectra were obtained by using a scanning spectrometer (Spex, Edison, NJ) at 543-nm excitation for Cy3 and at 630-nm excitation for Cy5. Transmission electron micrograph (TEM) samples were prepared by placing a drop of the nanoparticle aqueous solution onto a copper-coated Formvar-convered 300-mesh carrier grid for 30 s, before being wicked away and air-dried.

Oligonucleotide Microarray Fabrication. Probe printing solutions were prepared in a 2-fold dilution series from 50 to 6.25 μM in 1× TeleChem spotting solution. Oligonucleotide probes were arrayed onto SuperAldehyde slides using a PixSys 5500 robotic printer (Cartesian Technologies, Inc., Irvine, CA) in 60% relative humidity followed by incubation for 4 h. Before hybridization, the arrayed oligonucleotide microarrays were passivated by immersing in a solution containing 0.25 g of Na$_2$BH$_4$ dissolved in 75 mL of 1× PBS buffer and 25 mL of EtOH for 5 min. The slides were then washed three times in 0.2% SDS for 1 min and then in dH$_2$O for 1 min.

Hybridization Assays. A sandwich hybridization model was applied. Scheme 2 outlined the DNA hybridization procedures. The slides area spotted with oligonucleotide probes were placed with the Frame-Seal incubation chambers (9 × 9 mm), and 25 μL of mixed solution of target DNA samples diluted in 3× SSC, 40% formamide, and 0.2% SDS was pipetted into the incubation chambers. Hybridization was carried out for 6 h at 45 °C followed by washing with 1× SSC, 0.2% SDS; and 0.1× SSC, 0.2% SDS for 5 min each at ambient temperature. The secondary hybridization was then performed on DNA microarray slides either by applying 25 μL of the nanoparticle/DNA conjugates (containing 83 nM signaling probes in 1 × SSC, 0.2% SDS) into the frame chamber (step 3 in Scheme 2) or by applying 25 μL of cyanine dye-labeled signaling probes (83 nM signaling probes in 1× SSC, 0.2% SDS) into the frame chamber (step 4 in Scheme 2). The slide assembly was then shaken for 2 h at room temperature. After washing in 1× SSC, 0.2% SDS buffer twice for 5 min and then with 0.1× SSC for 30 s at ambient temperature, the slides were dried in air.

Microarray Imaging and Data Analysis. Microarrays were scanned at 10-μm resolution with the scanning laser confocal fluorescence microscope of a ScanArray 5000 system. The emitted fluorescent signal was detected by a photomultilier tube (PMT) at 570 nm for Cy3 and 670 nm for Cy5. For all microarray experiments, the laser power was 85% and the PMT gain was 75%. The fluorescent signals were analyzed by quantifying the pixel density (intensity) of each spot using ImaGene 3.0 (Biodiscovery, Inc., Los Angeles, CA). The local background signal was automati-

Scheme 2. Sandwich Hybridization Conducted on DNA Microarray[a]
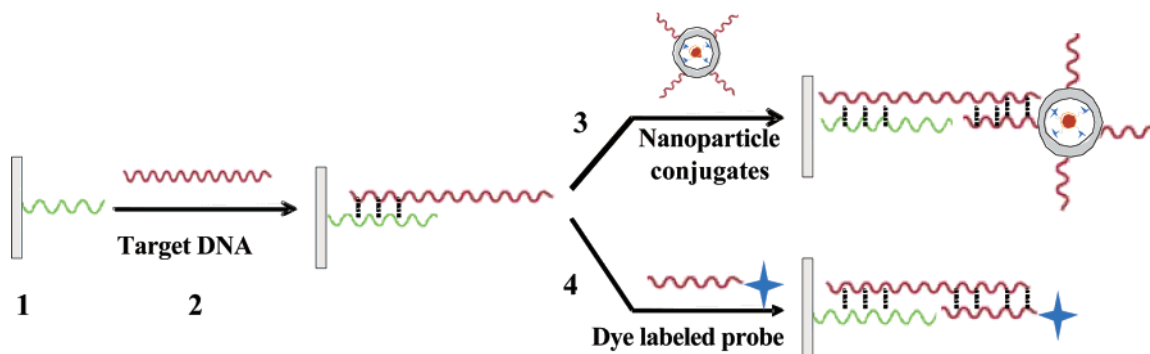
[a] (1) Oligonucleotide probes spotted on aldehyde slide; (2) oligonucleotide microarray hybridized with target sample; (3) hybridization with dye-doped nanoparticle/DNA conjugates; (4) hybridization with conventional dye-labeled probes.

cally subtracted from the hybridization signal of each separate spot, and the mean signal intensity of each spot was used for data analysis. Statistical analyses were performed using SigmaPlot 5.0 (Jandel Scientific, San Rafael, CA) or Microsoft Excel.

RESULTS AND DISCUSSION

Dye-Doped Au/Silica Core–Shell Nanoparticles and Their Conjugates Coupled with DNA Signaling Probes. The procedures for preparing the DNA capture probe functionalized silica nanoparticles that encapsulated with fluorophores are shown in Scheme 1. Cyanine dyes, i.e., Cy3 and Cy5, were selected for doping the nanoparticles because they are widely used as labeling in microarray technology due to their relatively high quantum yield and narrow emission band among the organic fluorophores. We used Au nanoparticles as a carrier for doping the organic fluorophore, which provided a well controlled, built-in mechanism whereby the fluorophore-labeled $(dT)_{20}$ probes are tailed on the Au nanoparticle surface by strong chemisorptions. This is an improvement in doping procedures compared with other procedures where the dyes were randomly embedded into the silica matrix,[12–14,24–26] or the dyes were physically adsorbed onto the Au surface in the doped Au/silica core–shell nanoparticles.[27–29] In our approach, the Au nanoparticles also work as hosts in the silica coating procedure, which produces silica core–shell nanoparticles with uniformed size distribution. The use of $(dT)_{20}$ as a spacer arm avoids the proximity of fluorophore to the Au surface, which effectively prevented quenching fluorescence by energy transfer.[22b,30] Finally, our approach ensures that the same amount of organic fluorophore is embedded onto each silica shell, which will result in good reproducibility when the prepared nanoparticles are used as labeling in the bioassay.

Full coverage of 15-nm Au nanoparticles with Cy5−oligomers were reported to contain up to 159 oligomer molecules per particle.[22a] To facilitate the generation of a silica shell on the Au nanoparticles, we adjusted the amount of dye-labeled $(dT)_{20}$ that was added to the Au colloid solution for a theoretical surface coverage of 70%. Experimental detection of the amount of dye-labeled $(dT)_{20}$ conjugated onto the Au nanoparticle was ~95 molecules per particle, which is ~65% of the theoretical coverage. This coverage was enough to prevent colloid aggregation in further experiments. To determine the coverage of dye-labeled $(dT)_{20}$, we used the DNase I to digest the $(dT)_{20}$ strands that were conjugated to the Au particle surface, thus releasing the fluorophore molecules to the solution. The surface coverage of the oligonucleotide on the Au colloid, which is equal to the surface coverage of the fluorophore molecules, was determined from the fluorescence of the solution. We also determined the coverage of the oligonucleotide according to the method of Demers et al.[22a] Mercaptoethanol (15 mM) was used to cleave the sulfur−gold bond, and then the entire conjugated DNA was released into solution and the fluorescence was determined, which resulted in 104 of $(dT)_{20}$ strands per Au particle being measured. These two methods gave close results in surface coverage determination. However, the method using DNase to digest the conjugated oligonucleotide is simpler and easier to handle.

Our objective was to synthesize gold/silica core−shell nanoparticles with a controlled amount of fluorophore molecules at the core−shell interface for subsequent application as labeling in microarray technology. The preparation of silica-coated Au nanoparticles has been reported by some research groups.[27–29] The general synthetic approach relies on the deposition of a thin silica shell by adsorption of organosilanes to the host colloidal gold, to preserve the colloidal stability during the whole sol−gel transition. Aminosilanes such as (3-aminopropyl)trimethoxysilane[32] and mercaptosilanes such as MPTS[19b,31] have been successfully used for this purpose. The organosilane binds to the nanoparticle surface, and silanols rapidly form upon alkoxide hydrolysis and condense during silica shell growth. The organosilane thus forms the interface between core and shell. Recently, Doering and Nie[31] reported the synthesis of dye-embedded core−shell nanoparticles with MPTS to form a uniform thin shell boundary. The growth of

(23) Guo, Z.; Guilfoyle, A.; Thiel, A.; Wang, R.; Smith, L. *Nucleic Acids Res.* **1994**, *22*, 5456−5465.

(24) (a) Taton, T. A.; Mirkin, C. A.; Letsinger, R. L. *Science* **2000**, *289*, 1757−1760. (b) Park, S. J.; Taton, T. A.; Mirkin, C. A. *Science* **2002**, *295*, 1503−1506.

(25) He, X. X.; Wang, K. M.; Tan, W. H.; Li, J.; Yang, X. H.; Huang, S. S.; Li, D.; Xiao, D. *J. Nanosci. Nanotechnol.* **2002**, *2*, 317−320.

(26) Yang, H. H.; Qu, H. Y.; Lin, P.; Li, S. H.; Ding, M. T.; Xu, J. G. *Analyst* **2003**, *128*, 462−466.

(27) Zhu, N. N.; Cai, H.; He, P. G.; Fang, Y. Z. *Anal. Chim. Acta* **2003**, *481*, 181−189.

(28) Chen, M. M. Y.; Katz, A. *Langmuir* **2002**, *18*, 8566−8572.

(29) Makarova, O. V.; Ostafin, A. E.; Miyoshi, H.; Norris, J. R.; Meisel, D. *J. Phys. Chem. B* **1999**, *103*, 9080−9084.

(30) Templeton, A. C.; Pietron, J. J.; Murray, R. W.; Mulvaney, P. *J. Phys. Chem. B* **2000**, *104*, 564−570.

(31) Doering, W. E.; Nie, S. M. *Anal. Chem.* **2003**, *75*, 6171−6176.

(32) (a) Liz-Marzan, L. M.; Giersig, M.; Mulvaney, P. *Langmuir* **1996**, *12*, 4329−4335. (b) Hall, S. R.; Davis, S. A.; Mann, S. *Langmuir* **2000**, *16*, 1454−1456.
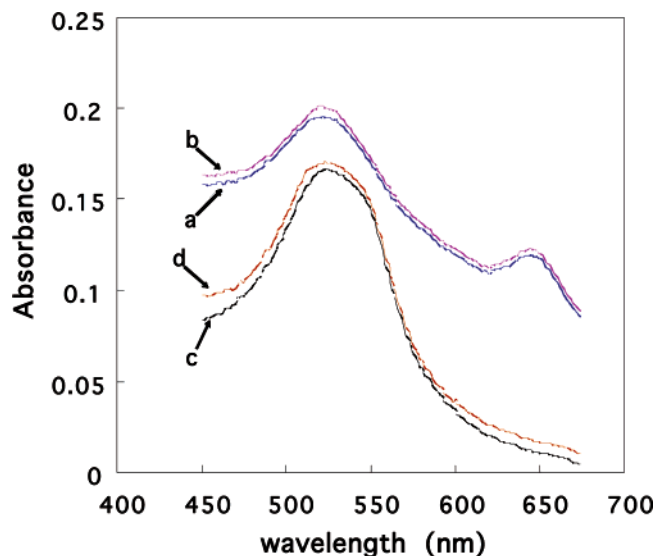
Figure 1. Optical spectra of Au colloid conjugated with cyanine dyes and the silica coated nanoparticles: (a) Cy5/Au nanoparticle conjugates; (b) silica-coated Cy5/Au nanoparticles; (c) Cy3/Au nanoparticle conjugates; (d) silica-coated Cy3/Au nanoparticles.

the Au nanoparticle was followed by procurement of a condensed silica layer with controllable thickness between 10 and 50 nm. We also found the formation of a uniform thin shell boundary ($\sim$5 nm) on the Au nanoparticle conjugated with dye at $\sim$65% surface coverage by using MPTS as precursor reagent. This initial shell was expanded by condensing of a mixture of silane of MPTS, (PEG)-silane, and TEOS to form a shell on the Au nanoparticle with a thickness of 10–15 nm and functionalized with thiol groups on the surface.[33] The thiol functional groups provided the active groups for covalent binding of DNA signaling probe whereas the PEG groups on the nanoparticle surface provide resistance to the nonspecific adsorption in a further hybridization bioassay. Figure 1 shows the absorption spectra of the silica-coated, dye-conjugated Au nanoparticles. The spectrum of the Au colloid contains the surface plasma band at 520 nm.[22] When Au nanoparticles are conjugated with Cy3-labeled (dT)$_{20}$, the gold plasma band shifts a little toward 526 nm, and the Cy3 fluorescence band at 570 nm overlaps with the surface plasma band at 526 nm (Figure 1, curve a). When Au nanoparticles were conjugated with Cy5-labeled (dT)$_{20}$, the Cy5 fluorescence band at 670 nm could be observed (Figure 1, curve c). In each case after coating with the silica shell, the absorption spectra of nanoparticles showed a slight increase in intensity of the Au plasma absorption band at $\sim$526 nm (Figure 1, curves b and d). This is consistent with the effects on absorption previously observed for silica-coated gold particles and is due to an increase in the local refractive index around the core–shell particles.[32] TEM measurement showed that the nanoparticles prepared by this method are spherical with uniform size of 40 $\pm$ 5 nm.

---

(33) During the formation of thin shell boundary with MPTS, some of the thiolated dye-labeled (dT)$_{20}$ may be stripped off from the Au colloid surface due to the competitive adsorption of MPTS with thiolated dye-labeled (dT)$_{20}$. However, these thiolated (dT)$_{20}$ stripped off from the Au colloid surface can be encapsulated into the silica shell formed by condensing of mixture of MPTS, (PEG)-silane, and TEOS because of the hydrophilic characteristics of the thiolated dye-labeled (dT)$_{20}$. Measurement of the fluorescence of the supernatant solution after the nanoparticle solution was centrifuged showed that less 1% of the conjugated thiolated dye-labeled (dT)$_{20}$ was in the solution.

Figure 2. Verification of oligonucleotide conjugation by gel electrophoresis. Right lane is the prepared Cy3-doped Au/silica nanoparticles and left lane is the DNA conjugates of Cy3-NP–Heme.

The presence of thiol functional groups and the PEG protection group in the silica corona of core–shell colloids prepared from mixtures of MPTS/TEOS/(PEG)-silane (1:1:1) mixture was confirmed by FT-IR spectroscopy. The FT-IR spectra exhibit peaks of C–H vibrations at 2934 cm^{-1}, R–SH vibrations at 2590–2550 cm^{-1}, and the strong bands centered at 1248 and 1150 cm^{-1} originate in the C–O–C bonds of PEG. The vibrational spectra also showed a weak Si–OH band at 955 cm^{-1} as well as Si–O–Si vibrations at around 1114 and 1003 cm^{-1} that were consistent with a shell of fully condensed siloxane centers.

In this work, the DNA signaling probes were directly coupled to the silica particles by using the heterobifunctional cross-linker sulfo-KMUS. Sulfo-KMUS is a water-soluble heterobifunctional cross-linker containing an extended aliphatic spacer. The sulfo-KMUS has a sulfohydroxysuccinimide (NHS) ester at one end, which reacts with a primary amine to form a stable amide bond, and a maleimide group at the other end, which reacts with a thiol to form a stable thioether bond. In the experiment, we used Denhardt's solution to block the nanoparticle surface to reduce the nonspecific adsorption of biomolecules by surface silanol groups and excess thiol groups. Transmission electron microscopy showed that the immobilization step did not result in aggregation. Fluorescence measurements also showed that the emission spectra and efficiencies of the nanoparticles coupled with the DNA probe were similar to that of the original dye-doped nanoparticles. The covalent coupling of DNA signaling probes onto the dye-doped nanoparticle surface was verified by gel electrophoresis as shown in Figure 2. The neutral dye-doped nanoparticles only slightly migrate through the gel (this can be attributed to unquenched silanol (SiOH) groups in the siloxane shell, which are negatively charged at pH 8–9). The dye-doped Au/silica

nanoparticle coupled with negatively charged oligonucleotides, however, results in substantially increased migration depending on the amount of oligonucleotides coupled to the nanoparticle. This result unambiguously ascertained the covalent coupling between the capture probes and the silica nanoparticle. The migration of DNA−nanoparticle conjugates shows a relatively broad band in the gel electrophoresis, which indicates the variation of numbers of DNA signaling probes coupled to the nanoparticle; however, the variation of DNA signaling probes associated with each nanoparticle would not affect the hybridization because a large volume of nanoparticle solution (25 μL) was used in hybridization and a prolonged hybridization time was applied. We estimated that ∼25 ± 4 oligonucleotide strands are associated with each silica nanoparticle by dividing the measured oligonucleotide concentration by the number of silica particles (3 independent measurements of the sample). This equals to the concentration of signaling probes at 83 nM in the final solution of DNA−nanoparticle conjugates. The average number of oligonucleotides coupled to nanoparticles depends on the properties of particle surface and coupling protocols, varied from 1 to 4 oligonucleotide strands per 10-nm silica-coated quantum dots,[19b,19c] 20 to 24 oligonucleotide strands per 2.6-nm CdS nanocrystal,[19d] and 1100 oligonucleotide strands per 70-nm silica nanoparticles.[27]

Oligonucleotide Microarrays Imaged with Dye-Doped Silica Core−Shell Nanoparticles. To explore the possibility of using dye-doped nanoparticles as labeling for microarray technology, we chose a 19-mer sequence specific to the *A. tolulyticus Td1* 16S gene and two 21-mer sequences specific to the *P. stutzeri* nitrite reductase gene and the *Nitrosospira sp. Np39-19* ammonia monooxygenase gene as the oligonucleotide probes with which to fabricate an oligonucleotide microarray on the aldehyde-functionalized slides. A random -sequenced probe was also spotted and served as the negative control. Three of 50-mer oligo templates that contain the complementary sequence to these probes respectively were used as targets. Sandwich hybridization detection was performed by staining the microarray with a mixture solution of Cy3-NP-Td1, Cy3-NP−Heme, Cy5-NP−Heme, and Cy5-NP−AmoA conjugates. The hybridization procedures are outlined in Scheme 2. Figure 3 displays the obtained two-color hybridization images. When the Cy3 (570 nm) and Cy5 (670 nm) channels were scanned, microarray spots containing probes of Heme and Td1 (Figure 3B), and Heme and AmoA (Figure 3C) were observed, respectively. At lower concentrations of probes in the spotting solution (6.25 and 12.5 μM), an increase of the fluorescence signal was observed until a saturation of the signal was reached at a high spotting concentration. Notice that the use of DNA/nanoparticle conjugates in hybridization showed negligible nonspecific adsorption in the random DNA probes that immobilized on the slide surface. The minimum of nonspecific adsorption of DNA/nanoparticle conjugates on the slide surface proved the effective blocking of the silica nanoparticle surface with the PEG groups bearing on nanoparticles and the blocking of Denhart's solution. PEG has been shown to be highly resistant to nonspecific adsorption to proteins while Denhart's solution is widely used as a blocking reagent for microarray slides to reduce nonspecific adsorption. Because of the similar surface structure between PEG and water, the DNA/nanoparticle conjugates containing the PEG groups also facilitate formation of Watson−

Crick base pairs during hybridization. The positive hybridization assays clearly demonstrated that the bioactivity of the DNA signaling probes is maintained despite the silica nanoparticles. Furthermore, the fluorescent intensities generated from Cy3-NP−Heme and Cy5-NP−Heme are equal and were found to correlate linearly with probes concentration, as shown in Figure 3D. These results also demonstrated that consistent and even hybridization can be obtained with the use of dye-doped silica core−shell nanoparticles as labeling reagents in multiplexed samples.

To investigate the improvement in sensitivity when using DNA−nanoparticle conjugates as labeling in microarray technology, we compared the detection of Heme−target DNA stained either by using Cy5-NP−Heme conjugates (Scheme 2, step 3) or the Cy5 directly labeled Heme-signaling probe (Scheme 2, step 4). For the purpose of comparing the sensitivity, the signaling probes applied in the two hybridization experiments were kept in same concentration (83 nM). Dose−response curves were generated by performing titration experiments in hybridization with seven concentrations (10^{-14}−10^{-7} M at 10-fold series dilution) of the Heme−target DNA. Figure 4A shows the dose−response curves of the Heme−target DNA with the two signaling approaches. The data resulted in sigmoid curves having linear ranges between approximately 5 pM and 10 nM for Cy5-NP−Heme and a linear range between approximately 50 pM amd 10 nM for Cy5−Heme signaling probe. The limit of detection (LOD), defined as the lowest concentration that yields a statistically distinguished fluorescent signal larger than backgrounds + 3 STD (standard deviations), is found to be ∼1 pM for the use of Cy5-NP−Heme as a label and 10 pM for the use of Cy5-Heme as a signal, as shown in Figure 4A. This LOD value by using prepared nanoparticles is competitive with the best prior values reported previously in DNA microarray technology as recorded for cyanine dye-based DNA microarray (LOD, 10−50 pM),[34] fluorescent nanocrystal-based DNA microarray (LOD, ∼2 nM),[19a] Au nanoparticle-based approaches (LOD ∼1 pM),[35] and chip-based microbead arrays (LOD, ∼0.1 pM).[36]

The use of the fluorophore-doped nanoparticles in microarray detection reveals 10-fold improvements in sensitivity and 1 order of magnitude extension of dynamic range compared to the direct use of cyanine dye. Although each silica nanoparticle was embedded with ∼100 cyanine dye molecules, only 10 times higher sensitivity improvement on microarray-based detection was achieved compared to detection by using conventional cyanine dye. The surface density of oligonucleotide probes immobilized on an aldehyde-functionalized slide was reported at 3 fmol/mm^2;[37] thus, the surface density of cyanine dye on the microarray spots is ∼1.8 fmol/mm^2 after hybridization by using dye-labeled signaling probes if 60% of hybridization efficiency was achieved (step 4, Scheme 2). In the case of using dye-doped nanoparticles as labeling in the hybridization (step 3, Scheme 2), a simple estimate indicates that ∼4 × 10^{10} close-packed silica nanoparticle could

(34) (a) Lipshutz, R. J.; Fodor, S. P. A.; Gingeras, T. R.; Lockhart, D. J. *Nat. Genet.* **1999**, *21*, 20−24. (b) Fodor, S. P. A. *Science* **1997**, *277*, 393.

(35) (a) Taton, T. A.; Lu, G.; Mirkin, C. A. *J. Am. Chem. Soc.* **2001**, *123*, 5164−5165. (b) Park, S.; Taton, T. A.; Mirkin, C. A. *Science* **2002**, *295*, 1503−1506.

(36) Ali, M. F.; Kirby, R.; Goodey, A. P.; Rodriguez, M. D.; Ellington, A. D.; Neikirk, D. P.; McDevitt, J. T. *Anal. Chem.* **2003**, *75*, 4732−4739.

(37) Zammatteo, N.; Jeanmart, L.; Hamels, S.; Courtois, S.; Louette, P. Hevesi, L.; Remacle, J. *Anal. Biochem.* **2000**, *280*, 143−150.
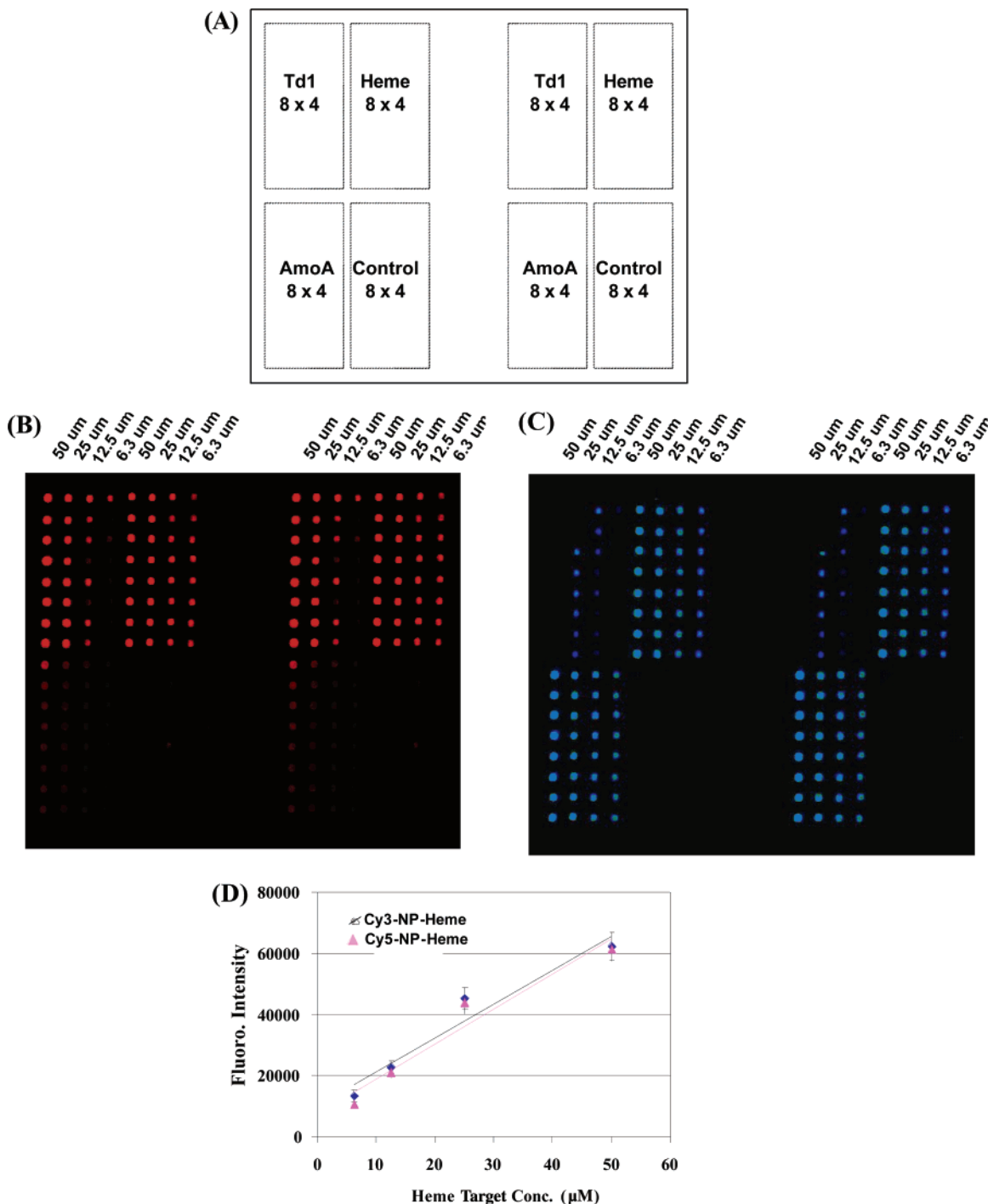
Figure 3. Display of two-color microarray images. The microarray composed of Heme, AmoA, Td1, and control probes in 16 × 8 megaformats, two replicates. Each probe was arrayed with four concentrations (prepared by 2-fold series dilution) in 8 × 4 formats (eight replicate spots per concentration). The slide was then hybridized with mixed-target samples of Td1−target, Heme−target, and AmoA−target at 100 pM each. After washing, the microarray was incubated with a mixture of equal amount of conjugates of Cy3-NP−Td1, Cy3-NP−Heme, Cy5-NP−Heme, and Cy5-NP−AmoA. Hybridization images were scanned after the slides were washed as described in the text. (A) The spatial illustration of probe assembly of the microarray; (B) image obtained via scanning at Cy3 channel; (C) image obtained via scanning at Cy5 channel; (D) correlation of fluorescent intensity generated from Cy3-NP−Heme and Cy5-NP−Heme on the spots that arrayed with Heme probes.

assemble on the 9 × 9 mm DNA microarray area. The application of 25 μL of 2 × 10^{12} particles mL^{-1} in the 9 × 9 mm frame chamber provided enough nanoparticles to form a close-packed particle layer on the microaray area. The surface density of dye molecules is estimated at ∼100 fmol/mm^2 considering close-packed 45-nm particles carrying ∼-95 dye molecules per particle. Thus, theoretically, the surface density of dye molecules is ∼50 times higher

by using the DNA−nanoparticle conjugates than by using the dye-labeled signaling probe in hybridization. The 10 times higher sensitivity improvement on our experimental results is reasonable considering the steric crowding effect in the hybridization event (e.g., ∼18% of densely packed layer of nanoparticles on microaray spot surface). The use of fluorescent nanocrystal−DNA conjugates in substrate-based DNA hybridization was reported to form ∼15%
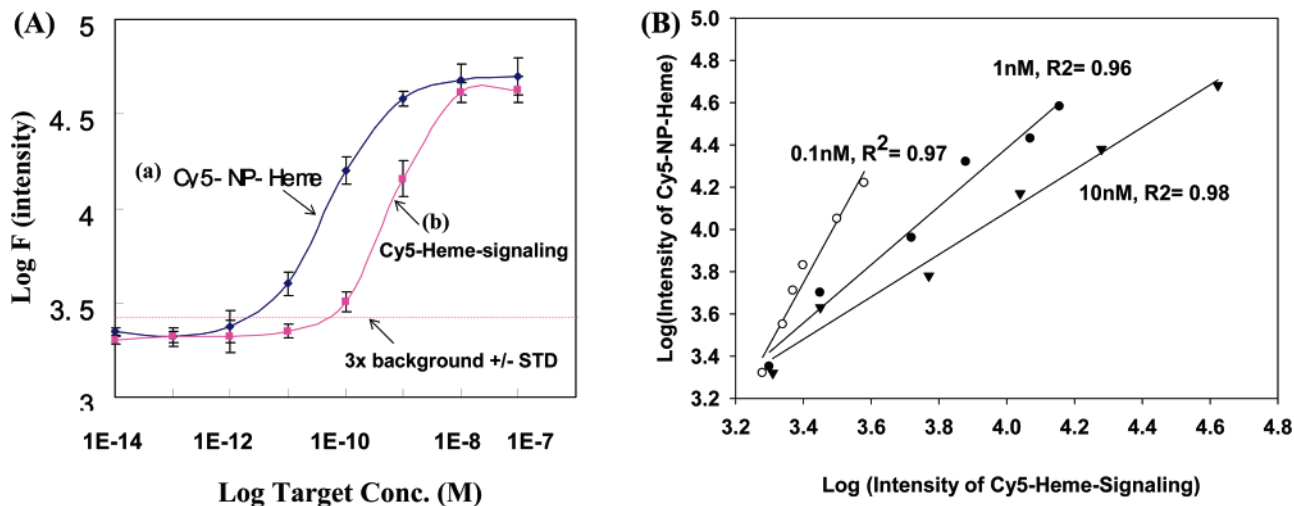
Figure 4. Quantitative evaluation of the model experiments as shown in Scheme 2. (A) Titration curves for sensitivity detected in sandwich assay by using (a) Cy5-NP−Heme as the signal reporter (Scheme 2, step 3); and (b) Cy5-Heme signaling as signal reporter (Scheme 2, step 4). The data shown represent mean ± standard deviation of 32 replicates from eight slides. (B) Correlation of fluorescence generated from different concentration of Cy5-NP−Heme and Cy5−Heme signaling in sandwich hybridization with three concentrations of Heme−target (0.1, 1, 10 nM).

densely packed layer of nanocrsytals on surface.[19c,19d] With no doubt, the sensitivity can be further improved by using dye-doped nanoparticles of smaller size which will increase the coverage of dye molecules in microarray spots. Moreover, comparison of the fluorescent intensity of DNA microarrays stained by using different concentrations of Cy5-doped nanoparticles and conventional Cy5 resulted in a very good correlation for different concentrations of target DNA, as shown in Figure 4B. This result indicated that even hybridization was achieved by using dye-doped nanoparticles as labeling.

Photostability of the Dye-Doped Nanoparticle. The photostability of the microarray signal was compared by continuously scanning the DNA microarray slides that employed Cy5-doped nanoparticles or Cy5 fluorophore as the label under a laser power of 85%. As shown in Figure 5, the signal intensity of the microarrays with Cy5-doped nanoparticles decreased to 95% of their initial intensities after nine continuous scans. However, the signal intensity of the microarrays with pure Cy5 as the label dropped to 76%. The results showed that the nanoparticles with the Cy5 dye embedded in the silica shell were more photostable than the conventional Cy5 label. The thin silica shell effectively protected the embedded Cy5 molecules from exposure to the environmental oxygen and ozone, which will cause dye degradation.[5] The higher photostability of the dye-doped nanoparticles made the bioassay more reproducible and accurate.

Discrimination of Single-Nucleotide Polymorphisms (SNPs) with Dye-Doped Nanoparticles. The detection of DNA sequence variations in the genomic DNA of different organisms is technically challenging, and the oligonucleotide microarray-based technology is one of the most promising methods for genotyping large numbers at low cost because of the high-throughput feature. We have evaluated the discrimination of single-nucleotide polymorphisms using the dye-doped nanoparticles as the labeling. For this purpose, microarrays composed of 15 of 21-mer oligomer probes having different sequences were fabricated on Superaldehyde slides. Oligomer Heme-A was fully complementary to part of the 50-mer Heme−target present in the

hybridization buffer. Oligomers Heme-B to Heme-D contained a single mismatched nucleotide in the middle with varying nucleo-
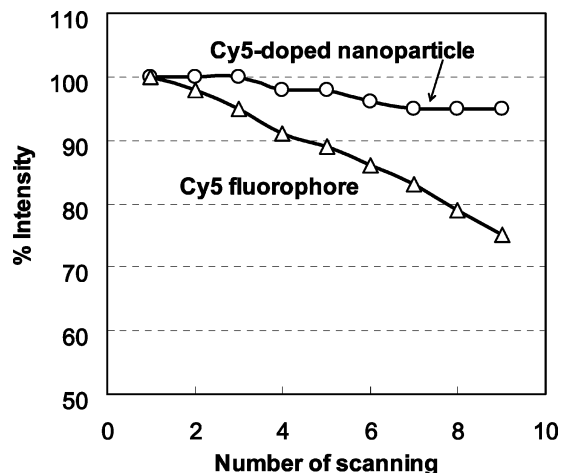

Figure 5. Comparison of signal photostabililty obtained by using Cy5-NP−Heme and Cy5−Heme signaling as the illuminating approaches in sandwich hybridization.

side type while oligomer Heme-E to oligomers Heme-J contained two mismatches in the middle with varying nucleoside types. Oligomers Heme-K to Heme-N contained three mismatches in the middle with varying nucleoside types, and oligomers Heme-O and Heme-P contained four and five mismatches, respectively. We carried out the experiments using Cy5-NP−Heme or Cy5-Heme signaling probes in sandwich hybridization. Under identical hybridization conditions, the resulting microarray images were analyzed and the discrimination factor F_m/F_p of each probe was determined, where F_m is the fluorescent intensity of mismatch probes and F_p the fluorescent intensity of the perfect match probe. Figure 6A and B showed the images obtained by hybridization with same concentration of Heme-target DNA and then stained by using Cy5-doped nanoparticles and conventional Cy5,
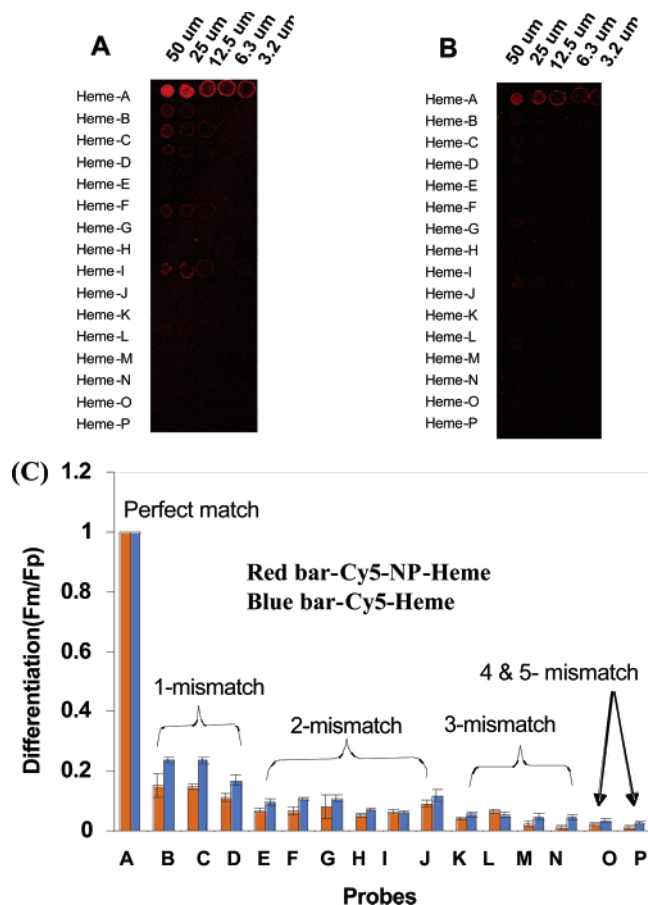
Figure 6. Determination of single-nucleotide polymorphism: (A) image display obtained in hybridization with 50 pM Heme−target and then imaged with Cy5-NP−Heme; (B) image display obtained in hybridization with 50 pM Heme−target and then imaged with Cy5−Heme signaling probe; (C) comparison of discrimination of nucleotide polymorphisms by using Cy5-NP−Heme and Cy5-Heme signaling probe. Data shown represent mean ± standard deviation of 24 replicates from three slides.

and Figure 6C compared the discrimination factor F_m/F_p of each probe as determined on the comparison experiments. The discrimination factor, F_m/F_p, which represents the signal ratio of the mismatch probes to perfect probes, is about $0.11-0.15$ for probes with a single-nucleotide mismatch when using Cy5-NP−Heme as labeling. In the case of using Cy5-Heme signaling probes, the F_m/F_p is $0.15-0.23$ for probes with a single-nucleotide mismatch. In other words, when using the dye-doped nanoparticles as the label, the signal intensity of the perfect match probe was ∼6−9 times higher than the intensities of probes with one mismatched nucleotide, whereas the signal intensity of the perfect match probe was ∼4−7 times higher than the probes with one mismatched nucleotide when using conventional Cy5 as label. The oligonucleotide probes containing three, four, and five mismatches showed almost no affinity for the target DNA due to the centralized position of three more mismatches, which also indicated that there was no nonspecific adsorption of Cy5-NP−Heme conjugates on the microarrays. The selectivity characteristics described here for the DNA microarray employing dye-doped nanoparticles are competitive with the best values reported

previously as recorded for different microarray detection approaches.[38]

As demonstrated above, the inclusion of the dye-doped nanoparticles in DNA microarray detection afforded attractive features such as high sensitivity and wide dynamic range, photostable signal, and high specificity to SNPs detection. Although only synthesized DNA fragments were used as target samples in the microarray-based sandwich hybridization by employing dye-doped nanoparticles at this stage, the dye-doped nanoparticles could also be used as labeling reagents for cDNA samples for gene expression analysis by adapting the indirect labeling strategy.[43] For example, cDNA samples can be synthesized by reverse transcriptase with primers containing specific capture sequences that can bind the signaling probe/nanoparticles conjugates through sequence complementarities. After the synthesized cDNAs are hybridized to microarrays, the bound cDNAs on the microararays can thus be detected by incubating the arrays with the signaling probe/nanoparticle conjugates.

CONCLUSION

We developed a new class of cyanine dye-doped Au/silica nanoparticles and demonstrated the first example of using the cyanine dye-doped nanoparticles as labeling for microarray-based detection. With an effective surface modification, nonspecific binding and aggregation of nanoparticles are minimized. The prepared dye-doped nanoparticles are stable in both aqueous electrolytes and organic solvents and provide highly fluorescent and photostable signals for bioanalysis. An order of magnitude increase in sensitivity enhancement and extension of dynamic range was achieved by using the cyanine dye-doped nanoparticles as labeling reagents in microarray detection. The use of dye-doped nanoparticles in a DNA microarray also improved the detection of single-base nucleotide polymorphism. The sensitivity of a microarray using dye-doped nanoparticles as the labeling reagents could be further improved by preparing smaller nanoparticles. It is also worth mentioning that the use of cyanine-doped nanoparticles as labeling in microarray technology can be directly applied to the currently available microarray scanner that found in most biological laboratory without setting up a new scanner system.

(38) The discrimination of SNPs on a DNA microarray depends on the length of the oligonucleotide probes, the position of mismatched nucleoside in the probe sequence, and hybridization models applied as well as hybridization conditions. For example, the ratios of perfect match probe to single-nucleotide mismatch probes have been reported as $2.5-100$ for various 17-mer probes arrayed on polyacrylamide gel pads;[39] ∼2 for a 15-nucleotide sequence on bead fiber-optic microarray;[40] 5.4 for 25-mer, 4.3 for 30-mer, and 3.3 for 35-mer oligonucleotide probes on aminosilane slides;[41] and $6-3$ for 15-mer probes in Affymatrix GeneChips generated by light-directed chemical synthesis.[42]

(39) Mikhailovich, V.; Lapa, S.; Gryadunov, D.; Sobolev, A.; Strizhkov, B.; Chernyh, N.; Skotnikova, O.; Irtuganova, O.; Moroz, A.; Litvinov, V.; Vladimirskii, M.; Perelman, M.; Chernousova, L.; Erokhin, V.; Zasedatelev, A.; Mirzabekov, A. *J. Clin. Microbiol.* **2001**, *39*, 2531−2540.

(40) Ferguson, J. A.; Steemers, F. J.; Walt, D. R. *Anal. Chem.* **2000**, *72*, 5618−5624.

(41) Relogio, A.; Schwager, C.; Richter, A.; Ansorge, W.; Valcarcel, J. *Nucleic Acids Res.* **2002**, *30*, e51.

(42) Chee, M.; Yang, R. Hubbell, E.; Berno, A.; Huang, X. C.; Stern, D.; Winkler, J.; Lockhart, D. J.; Morris, M. S.; Fodor, S. P. A. *Science* **1996**, *274*, 610−614.

(43) (a) Zhou, J. Z.; Thompson, D. K.; Xu, Y.; Tiedje, J. M. *Microabial Functional Genomics*; John Willey & Sons: Hoboken, NJ, 2004. (b)Yu, J. D.; Othman, M. I.; Farjo, R.; Zareparsi, S.; MacNee, S. P.; Yoshida, S.; Swaroop, A. *Mol. Vis.* **2002**, *8*, 130−137.